J|A|C|S
ARTICLES
Published on Web 12/19/2003

Protein-Template-Driven Formation of Polynuclear Iron Species†

Simon A. Malone,[‡,§] Allison Lewin,[‡] Mehmet A. Kilic,[||,⊥] Dimitri A. Svistunenko,[▽] Chris E. Cooper,[▽] Michael T. Wilson,[▽] Nick E. Le Brun,[‡] Stephen Spiro,[||] and Geoffrey R. Moore*[,‡]

Contribution from the Schools of Chemical Sciences and Pharmacy and of Biological Sciences, University of East Anglia, Norwich NR4 7TJ, U.K., and Department of Biological Sciences, Central Campus, University of Essex, Colchester CO3 4SQ, U.K.

Received June 3, 2003; E-mail: g.moore@uea.ac.uk

Abstract: Ferritins are iron-storage proteins capable of holding up to 4500 Fe^{3+} ions within a single water-soluble protein shell made from 24 polypeptide chains. The Glu128Arg/Glu135Arg mutants of *Escherichia coli* and *Rhodobacter capsulatus* bacterioferritins are unable to associate into 24-meric structures, with dimers of polypeptide chains being their stable forms. The aerobic addition to these of up to 8−10 or 14−20 Fe^{2+} ions per dimer, respectively, results in the oxidation of the added Fe^{2+} to Fe^{3+}. Gel permeation chromatography and sedimentation equilibrium studies confirm that the Fe^{3+} ions are associated with the polypeptide dimer, and the lack of intense EPR signals from magnetically isolated Fe^{3+} ions confirms the formation of one or more antiferromagnetically coupled clusters of Fe^{3+} ions. The effect of Fe^{3+} chelators on iron-loaded subunit dimers is to remove the Fe^{3+} from the protein, but to do so slowly, consistent with it not being merely adventitiously associated with protein. These data provide experimental support for the presence of nucleation centers for the mineral cores in bacterioferritins and indicate that these proteins are not simply acting as vessels in which hydrolysis of Fe^{3+} occurs independent from the protein surface. From analyses of X-ray structures and amino acid sequence comparisons, possible nucleation sites are identified.

Introduction

The aqueous chemistry of Fe^{2+} in the presence of O_2 is dominated by its oxidation to Fe^{3+} and the hydrolytic formation of insoluble polynuclear hydroxide species.[1−4] The complexity of this chemical behavior is a major reason for the widespread use of nonaqueous solvents for the synthesis of polynuclear iron-containing coordination compounds,[4−9] though there has been some success with synthetic procedures employing aqueous solutions.[10,11] An aim of many of these synthetic studies, whether water-based or not, is to provide insight into polynuclear iron species that may have relevance to iron-containing proteins,[3,4,12−15] such as the diiron enzymes ribonucleotide reductase and methane monooxygenase, and the ferritin family of iron-storage proteins. Determination of the structure and mechanism(s) of formation of the major iron component(s) of ferritins is a particularly challenging topic that has led to the work described in this paper.

Ferritins[15−20] generally consist of 24 polypeptide chains of 18−21 kDa each, which associate to create an approximately spherical shell of 20−25 Å thickness that surrounds a cavity of ∼80 Å diameter.[16] An iron mineral, the core, can be formed in this central cavity, which has the capacity to accommodate ∼4500 Fe^{3+} ions as ferrihydrite,[15,19] with an average composi-

† Abbreviations: BFR, bacterioferritin; DFO, desferrioximine; HoSF, horse spleen ferritin; PCR, polymerase chain reaction; LB, Luria Bertani; IPTG, isopropyl α-D-thiogalactopyranoside; PMSF, phenylmethylsulfonyl fluoride; HEPES, *N*-2-hydroxyethylpiperazine-*N*′-2-ethanesulfonic acid; MES, 2-(*N*-morpholino)ethanesulfonic acid; MOPS, 3-(*N*-morpholino)-propanesulfonic acid; Tiron, 4,5-dihydroxy-1,3-benzenedisulfonic acid.

‡ School of Chemical Sciences and Pharmacy, University of East Anglia.
§ Present address: University of Manchester, Oxford Rd., Manchester M13 9PL, U.K.
|| School of Biological Sciences, University of East Anglia.
⊥ Present address: Akdeniz University, Dumlupinar Bulvari, 07058 Kampus, Antalya, Turkey.
▽ University of Essex.

(1) Flynn, C. M. *Chem. Rev.* **1984**, *84*, 31−41.
(2) Richens, D. T. *The Chemistry of Aqua Ions*; Wiley: Chichester, U.K., 1997; pp 365−385.
(3) Schneider, W. *Chimia* **1988**, *42*, 9−20.
(4) Lippard, S. J. *Angew. Chem., Int. Ed. Engl.* **1988**, *27*, 344−361.
(5) Dong, Y. H.; Ménage, S.; Brennan, B. A.; Elgren, T. E.; Jang, H. G.; Pearce, L. L.; Que, L., Jr. *J. Am. Chem. Soc.* **1993**, *115*, 1851−1859.
(6) Taft, K. L.; Papaefthymiou, G. C.; Lippard, S. J. *Inorg. Chem.* **1994**, *33*, 1510−1520.
(7) Micklitz, W.; McKee, V.; Rardin, R. L.; Pence, L. E.; Papaefthymiou, G. C.; Bott, S. G.; Lippard, S. J. *J. Am. Chem. Soc.* **1994**, *116*, 8061−8069.
(8) Caneschi, A.; Cornia, A.; Fabretti, A. C.; Gatteschi, D. *Angew. Chem., Int. Ed. Engl.* **1995**, *34*, 2716−2718.
(9) Benelli, C.; Parsons, S.; Solan, G. A.; Winpenny, R. E. P. *Angew. Chem., Int. Ed. Engl.* **1996**, *35*, 1825−1828.
(10) Wieghardt, K.; Pohl, K.; Jibril, I.; Huttner, G. *Angew. Chem., Int. Ed. Engl.* **1984**, *23*, 77−78.
(11) Heath, S. L.; Powell, A. K. *Angew. Chem., Int. Ed. Engl.* **1992**, *31*, 191−193.
(12) Shu, L.; Nesheim, J. C.; Kauffmann, K.; Münck, E.; Lipscomb, J. D.; Que, L., Jr. *Science* **1997**, *275*, 515−518.
(13) Hwang, J.; Krebs, C.; Huynh, B. H.; Edmondson, D. E.; Theil, E. C.; Penner-Hahn, J. C. *Science* **2000**, *287*, 122−125.
(14) Hagen, K. S. *Angew. Chem., Int. Ed. Engl.* **1992**, *31*, 1010−1012.
(15) Powell, A. K. *Struct. Bonding* **1997**, *88*, 1−38.
(16) Harrison, P. M.; Arosio, P. *Biochim. Biophys. Acta* **1996**, *1275*, 161−203.
(17) Le Brun, N. E.; Thomson, A. J.; Moore, G. R. *Struct. Bonding* **1997**, *88*, 103−108.
(18) Chasteen, N. D. *Met. Ions Biol. Syst.* **1998**, *35*, 479−514.

 10.1021/ja036483z CCC: $27.50

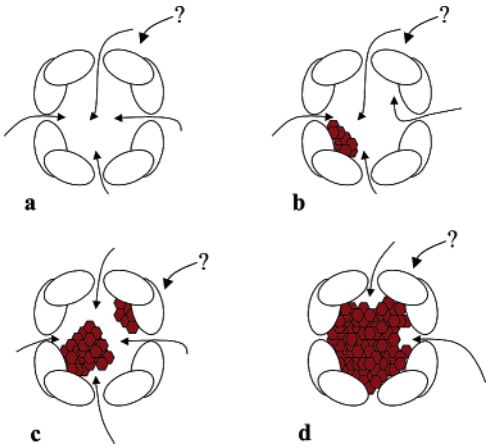

Figure 1. Crystal growth mechanism of core formation in ferritins (after Clegg et al.[24]). The arrows indicate the passage of Fe^{2+} ions into the cavity. The arrows with question marks refer to Fe^{2+} binding and being oxidized at the ferroxidase centers. It has not been established whether occupation of the ferroxidase center occurs with Fe^{2+} binding from the outside of the 24-mer or via the surface of the central cavity, and it is not clear that Fe^{2+} oxidized at the bacterioferritin ferroxidase centers enters the central cavity and becomes part of the core. The diagram shows the crystal growth occurring by incoming Fe^{2+} being oxidized on the surface of the growing crystallite, as summarized by Clegg et al.[24] However, the accretion hierarchy has not been firmly established, and some incoming Fe^{2+} may displace Fe^{3+} at the protein surface.

tion of $(FeOOH)_8FeO{\cdot}H_2PO_4$. The iron probably enters and exits the cavity via channels in the surrounding protein shell that are formed at the interfaces between the associated polypeptide chains.[16,18,20] *Listeria innocua* ferritin is unusual in that it consists of only 12 subunits with a central cavity of ~40 Å diameter, which enables it to hold ~500 Fe^{3+} ions.[21] This 12-mer ferritin has a structure similar to that of the DNA-binding protein from starved *Escherichia coli* cells (Dps),[22] which can also hold ~500 Fe^{3+} ions.[23] Core formation in ferritins is poorly understood, partly because there are major technical problems in determining the identity of the core and the chemical details of the steps leading to its formation. The crystal growth mechanism[24] summarized in Figure 1 illustrates some of the problems. In the early stage of reaction a protein shell may contain several nucleation centers, but core formation becomes dominated by one such center. This means that preparations of iron-containing ferritins may be monodisperse with regard to their protein components but polydisperse in their core components. It also means that, at relatively low iron:protein ratios, large clusters can be formed in some of the protein shells.[16,18,25−27] A consequence of the polydisperse nature of the cores is that, in crystals of ferritin, though the protein shell is ordered the iron-containing core is not.[19] Consequently, the structure of the core mineral has not been determined by X-ray crystallography, and complete structural and mechanistic characterization of intact ferritins containing 24 subunits may not be possible. For this reason attempts have been made to dissociate the protein shells of 24-mer ferritins with some retention of Fe^{3+}-core-formation activity. However, disaggregation of the wild-type oligomers into monodisperse smaller structures is only possible by the addition of denaturants, and these cause the subunits themselves to denature with the loss of core-forming activity.[28−32] Hence, attempts to stabilize subunit dimer forms of ferritins so that they do not associate into 24-meric shells have been made by site-directed mutagenesis and chemical modifications.[33,34] The Fe^{3+}-binding properties of two of these engineered proteins, the bacterioferritins from *E. coli* and *Rhodobacter capsulatus*, are described in this paper.

Bacterioferritin (BFR) is unique among the ferritin family in containing 12 intersubunit heme groups per 24-mer,[17,35] though these do not[36] play a role in the aerobic oxidative uptake of Fe^{2+}. BFR also has intrasubunit dinuclear iron centers, called ferroxidase centers,[17,36−39] which are required for rapid utilization of Fe^{2+} to form the Fe^{3+}-containing core. This aerobic oxidative uptake of Fe^{2+} by BFR takes place in at least three steps: First, pairs of Fe^{2+} ions bind to the ferroxidase centers. This is followed by their oxidation to Fe^{3+}. In the third phase, deposition of iron as ferric oxide in the BFR cavity occurs.[17,40,41] A functional ferroxidase center is required for all three phases to occur at a fast rate under normal conditions. From the X-ray structure of *E. coli* BFR,[38] we proposed that contacts between Glu128 and Glu135 of one subunit and Arg61 and the N-terminal amine, respectively, of neighboring subunits would be critical for assembly of a 24-mer. We substituted Glu128 and Glu135 of *R. capsulatus* BFR with arginine and found that the resulting protein was a monodisperse dimeric species of ~36−40 kDa which retained ferroxidase activity.[34,42] In the present paper we describe the formation and properties of the *E. coli* Glu128Arg/Glu135Arg mutant BFR, which is also a stable subunit dimer that has ferroxidase activity, and results of investigations with gel permeation chromatography, analytical ultracentrifugation, and UV−vis and EPR spectroscopies that

(19) Ford, G. C.; Harrison, P. M.; Rice, D. W.; Smith, J. M. A.; Treffry, A.; White, J. L.; Yariv, J. *Philos. Trans. R. Soc. London* **1984**, *B304*, 551−565.
(20) Jin, W.; Takagi, H.; Pancorbo, B.; Theil, E. C. *Biochemistry* **2001**, *40*, 7525−7532.
(21) Ilari, A.; Stefanini, S.; Chiancone, E.; Tsernoglou, D. *Nat. Struct. Biol.* **2000**, *7*, 38−43.
(22) Grant, R. A.; Filman, D. J.; Finkel, S. E.; Kolter, R.; Hogle, J. M. *Nat. Struct. Biol.* **1998**, *5*, 294−303.
(23) Ilari, A.; Ceci, P.; Ferrari, D.; Rossi, G. L.; Chiancone, E. *J. Biol. Chem.* **2002**, *277*, 37619−37623.
(24) Clegg, G. A.; Fitton, J. E.; Harrison, P. M.; Treffry, A. *Prog. Biophys. Mol. Biol.* **1980**, *36*, 53−86.
(25) Bauminger, E. R.; Harrison, P. M.; Nowik, I.; Treffry, A. *Biochemistry* **1989**, *28*, 5486−5493.
(26) Bauminger, E. R.; Harrison, P. M.; Hechel, D.; Hodson, N. W.; Nowik, I,; Treffry, A.; Yewdall, S. J. *Biochem. J.* **1993**, *296*, 709−719.
(27) Perieira, A. S.; Tavares, P.; Lloyd, S. G.; Danger, D.; Edmondson, D. E.; Theil, E. C.; Huynh, B. H. *Biochemistry* **1997**, *36*, 7917−7927.
(28) Listowsky, I.; Blauer, G.; Englard, S.; Betheil, J. J. *Biochemistry* **1972**, *11*, 2176−2181.
(29) Crichton, R. R.; Bryce, C. F. A. *Biochem. J.* **1973**, *133*, 289−299.
(30) Stefanini, S.; Vecchini, P.; Chiancone, E. *Biochemistry* **1987**, *26*, 1831−1837.
(31) Stefanini, S.; Cavallo, S.; Wang, C.-Q.; Tataseo, P.; Vecchini, P.; Giartosio, A.; Chiancone, E. *Arch. Biochem. Biophys.* **1996**, *325*, 58−64.
(32) Santambrogio, P.: Pinto, P.; Levi, S.; Cozzi, A.; Rovida, E.; Albertini, A.; Artymiuk, P.; Harrison, P. M.; Arosio, P. *Biochem. J.* **1997**, *322*, 461−468.
(33) Levi, S.; Santambrogio, P.; Albertini, A.; Arosio, P. *FEBS Lett.* **1993**, *336*, 309−312.
(34) Kilic, M.; Spiro, S.; Moore, G. R. *Protein Sci.* **2003**, *12*, 1663−1674.
(35) Stiefel, E. I.; Watt, G. D. *Nature* **1979**, *279*, 81−83.
(36) Andrews, S. C.; Le Brun, N. E.; Barynin, V.; Thomson, A. J.; Moore, G. R.; Guest, J. R.; Harrison, P. M. *J. Biol. Chem.* **1995**, *270*, 23268−23274.
(37) Le Brun, N. E.; Andrews, S. C.; Guest, J. R.; Harrison, P. M.; Moore, G. R.; Thomson, A. J. *Biochem J.* **1995**, *312*, 385−392.
(38) Frolow, F.; Kalb, A. J.; Yariv, J. *Nat. Struct. Biol.* **1994**, *1*, 453−460.
(39) Macedo, S.; Romão, C. V.; Mitchell, E.; Matias, P. M.; Liu, M. Y.; Xavier, A. V.; LeGall, J.; Teixeira, M.; Lindley, P.; Carrando, M. A. *Nat. Struct. Biol.* **2003**, *10*, 285−290.
(40) Le Brun, N. E.; Wilson, M. T.; Andrews, S.; Guest, J. R.; Harrison, P. M.; Thomson, A. J.; Moore, G. R. *FEBS Lett.* **1993**, *333*, 197−202.
(41) Yang, X.; Le Brun, N. E.; Thomson, A. J.; Moore, G. R.; Chasteen, N. D. *Biochemistry* **2000**, *39*, 4915−4923.
(42) Spiro, S.; Kilic, M.; Lewin, A.; Dobbin, S.; Thomson, A. J.; Moore, G. R. In *Iron Metabolism, Inorganic Biochemistry and Regulatory Mechanisms*; Ferreira, G. C., Moura, J. J. G., Franco, R., Eds.; Wiley-VCH: Weinheim, Germany, 1999; pp 211−226.

show that each dimer *R. capsulatus* BFR molecule in aqueous solution acts as a template for Fe^{2+} oxidation and accumulates 14−20 Fe^{3+} ions per molecule in one or more polynuclear clusters. In contrast to this, the *E. coli* bacterioferritin dimer is shown to accumulate only 8−10 Fe^{3+} ions per molecule, which provides some insight into the early stages of polynuclear iron cluster formation. We chose to study engineered forms of both *E. coli* and *R. capsulatus* BFRs because at the outset of our work these were the only 24-mer BFRs whose three-dimensional structures had been determined,[38,43] because they have different surface charges on the inner surfaces of their central cavities (see later), and because we had overexpression systems for both[17,44] and had shown that they were both capable of accumulating a large polynuclear iron core.[17,45] An approach to modeling the iron cores of ferritins very different from the synthetic chemistry methodologies alluded to earlier[4−11] and the protein-based approach described in this paper are the controlled hydrolysis of Fe^{3+}-containing solutions with citric acid[46,47] and the formation of carbohydrate−Fe^{3+} complexes.[48,49] Both of these latter approaches have yielded large polynuclear iron cores, and though their subsequent structural characterization has not been reported, EXAFS and ^{57}Fe Mössbauer spectroscopic data show that the mineral components of the carbohydrate−Fe^{3+} complexes resemble those of ferritins.[48,49]

Experimental Section

The genes for the Glu128Arg/Glu135Arg and Met52Ala/Glu128Arg/Glu135Arg mutants of *R. capsulatus* BFR were constructed by PCR mutagenesis,[50] cloned into pET21a (Novagen), and expressed in *E. coli* MAK96 (BL21 Δ*bfr*),[42] and the gene for the Glu128Arg/Glu135Arg mutant of *E. coli* BFR was similarly constructed and expressed in the same strain. The nucleotide sequences of the mutated genes were confirmed by DNA sequencing and by determination of the molecular weights of their corresponding proteins using mass spectrometry, and their expression was induced as previously described.[44] The *R. capsulatus* BFR subunit dimers were purified by chromatography of the cell-free extract on a Q-Sepharose anion exchange column (50 mM potassium phosphate buffer, pH 7.2, eluted with a NaCl gradient at 0.22 M NaCl) followed by chromatography on a S-100 HR gel filtration column (50 mM potassium phosphate buffer, pH 7.2). The *E. coli* BFR subunit dimer precipitated after release from the cells by sonication at 4 °C (50 mM HEPES buffer, pH 7.2, 50 mM NaCl, 1 mM PMSF). The precipitate was recovered by centrifugation and redissolved in a minimum volume of BFR buffer (20 mM HEPES, 100 mM KCl, 0.1 mM EDTA, 10% (v/v) glycerol, pH 7.8). The sample was then loaded onto a DEAE-Sepharose anion exchange column (Pharmacia) equilibrated with BFR buffer, the column washed with BFR buffer, and the BFR subunit dimer eluted with BFR buffer containing 300 mM KCl. The fractions containing BFR subunit dimer were pooled, and the protein was precipitated with 80% (w/v) ammonium sulfate, redissolved in a minimum volume of BFR buffer, and applied to a Sephacryl S300-HR or Superdex S75 column (Pharmacia) equilibrated with the same buffer in its final purification step. Electrospray ionization mass spectrometry (ESI-MS) of the purified proteins gave masses consistent with the expected amino acid sequences. ESI-MS was carried out with a Micromass platform I mass spectrometer calibrated with horse heart myoglobin. The solvent used was 1:1 acetonitrile and water containing 0.1% formic acid, and samples were run at a flow rate of 20 μL min^{-1}. UV−vis electronic absorption spectra were collected with Perkin-Elmer Lambda 800 and 900 and Hitachi U2000 and U3000 spectrophotometers. Nonheme iron was determined as the [Fe^{2+}(ferrozine)$_3$] complex on the basis of the method of Stookey.[51] The average level of iron loading was found to be 0−10 Fe^{3+} ions per molecule for the *R. capsulatus* subunit dimer as prepared and ≪1 Fe^{3+} ion per molecule after treatment to remove nonheme iron. Iron-free BFR subunit dimers were prepared by anaerobic dialysis of the isolated protein against 100 mM sodium acetate (pH 4.2) at 4 °C and then dialysis against 100 mM sodium EDTA (pH 7.0), followed by dialysis against the required buffer as described previously[52] or through anaerobic dialysis of the isolated protein against 100 mM HEPES (pH 7) at 4 °C and treatment with 2,2′-bipyridyl and sodium dithionite.

Heme contents were determined using the Soret absorbance bands of the nonheme iron free proteins;[37,45] $\epsilon_{419} = 1.4 \times 10^5$ M^{-1} cm^{-1} for *R. capsulatus* BFR, and $\epsilon_{418} = 1.09 \times 10^5$ M^{-1} cm^{-1} for *E. coli* BFR. As prepared, *R. capsulatus* Glu128Arg/Glu135Arg BFR and Met52Ala/Glu128Arg/Glu135Arg BFR contained 0.05−0.7 and 0 heme groups per dimer, respectively, and *E. coli* Glu128Arg/Glu135Arg BFR up to 0.3 heme group per subunit dimer. Fully heme loaded *E. coli* Glu128Arg/Glu135Arg BFR in 0.1 M MES (pH 6.5) was obtained following addition of freshly prepared hemin chloride and the removal of adventitious heme by passage of the sample through a PD-10 column (Pharmacia) equilibrated with 0.1 M MES (pH 6.5). Aqueous solutions of Fe^{2+} ions were prepared fresh for each experiment from solid $Fe(NH_4)_2(SO_4)_2 \cdot 6H_2O$. Stock solutions of Fe^{2+} were degassed with Ar or N_2, and a gastight Hamilton syringe was used for all additions to aerobic solutions of BFR subunit dimer. The average iron content per fully loaded subunit dimers was determined by titrating Fe^{2+} into the apoproteins at pH 6.5 (0.1 M MES) and pH 7.0 (0.1 M MOPS) until the protein began to precipitate, as judged by a drop in absorbance at 280 nm, removing precipitated material by centrifugation at 14000 rpm for 10 min, and determining the iron content of the remaining soluble protein. In some experiments the Fe^{2+}/protein mixtures were incubated at 25 °C for 4 h to ensure complete oxidation of the added Fe^{2+}, centrifuged at 14000 rpm for 10 min to remove precipitated iron-containing species, and passed through a PD-10 column (Pharmacia) equilibrated with 0.1 M MES (pH 6.5) to remove adventitious iron, and the nonheme Fe^{3+} content of the eluted protein was determined.

A calibrated Sephacryl S100 HR column (90 cm × 4 cm) was used for the molecular weight determinations. The column was calibrated using Sigma gel filtration calibration kit GF-1000, and run with 100 mM MES buffer (pH 6.5). Loading was by manual injection with an injection volume of 1 mL, the elution rate was 0.25 mL min^{-1}, and 2.5 mL fractions were collected. Analytical ultracentrifugation measurements at 15000−20000 rpm were made at 20 °C with a Beckman-Coulter Optima XL/I analytical ultracentrifuge and an An50Ti rotor. Samples contained 2−8 μM subunit dimer in 0.1 M MES (pH 6.5). Each experiment was done at three different protein concentrations and three different speeds. All conditions gave very similar results. Standard double-sector cells were used with a sample volume of 110 μL and reference volume of 116 μL. The absorbance at 280 nm across the cell was measured at intervals of 2−4 h to ensure the system reached equilibrium. The molecular weight, M_r, was

(43) Cobessi, D.; Huang, L.-S.; Ban, M.; Pon, N. G.; Daldal, F.; Berry, E. A. *Acta Crystallogr.* **2002**, *D58*, 29−38.
(44) Penfold, C. N.; Ringeling, P. L.; Davy, S. L.; Moore, G. R.; McEwan, A. G.; Spiro, S. *FEMS Microbiol. Lett.* **1996**, *139*, 143−148.
(45) Ringeling, P. L.; Davy, S. L; Monkara, F. A.; Hunt, C.; Dickson, D. P. E.; McEwan, A. G.; Moore, G. R. *Eur. J. Biochem.* **1994**, *223*, 847−855.
(46) Spiro, T. G.; Allerton, S. E.; Renner, J.; Terzis, A.; Bils, R.; Saltman, P. *J. Am. Chem. Soc.* **1966**, *88*, 2721−2726.
(47) Spiro, T. G.; Pape, L.; Saltman, P. *J. Am. Chem. Soc.* **1967**, *89*, 5555−5559.
(48) Theil, E. C.; Sayers, D. E.; Brown, M. A. *J. Biol. Chem.* **1979**, *254*, 8132−8134.
(49) Yang, C.-Y.; Bryan, A. M.; Theil, E. C.; Sayers, D. E.; Bowen, L. H. *J. Inorg. Biochem.* **1986**, *28*, 393−405.
(50) Hutchings, M. I.; Shearer, N.; Wastell, S.; van Spanning, R. J. M.; Spiro S. *J. Bacteriol.* **2000**, *182*, 6434−6439.
(51) Stookey, L. L. *Anal. Chem.* **1970**, *42*, 779−781.
(52) Bauminger, E. R.; Harrison, P. M.; Hechel, D.; Nowik, I.; Treffry, A. *Biochim. Biophys. Acta* **1991**, *1118*, 48−58.

determined by fitting data to the equation

$$A_r = A_{r_0} \exp\{[M_r(1 - \upsilon\rho)\omega^2(r^2 - r_0^2)]/2RT\}$$

where ω is the angular velocity, υ the partial specific volume of the solute, and ρ the solvent density. During the fitting procedure values of 0.73 mL/g and 1 g/mL were used for υ and ρ, respectively. For the analysis of the iron-bound samples, an attempt was made to adjust the value of υ to compensate for the iron particle(s), on the basis of a density of 3.96 g/mL for ferrihydrite.[53] However, due to the small contribution of the Fe^{3+} component to the mass of the Fe^{3+}-loaded subunit dimer, this correction resulted in an insignificant variation to the calculated sedimentation profile of the Fe^{3+}-loaded subunit dimer.

The ease of removal of product Fe^{3+} resulting from the oxidation of Fe^{2+} ions added to the subunit dimers was determined from the time dependence of the formation of Fe^{3+}−Tiron complexes. A final concentration of 60 μM Fe^{2+} was added to 0.5 μM *E. coli* wild-type BFR (giving 120 Fe atoms per 24-mer), 6.0 μM *E. coli* Glu128Arg/Glu135Arg BFR (10 Fe atoms per dimer), and a protein-free control, all three in 0.1 M MES buffer (pH 6.5) at 25 °C. Iron oxidation was measured by monitoring the absorbance at 340 nm, and when oxidation was complete, the protein samples were passed through a PD10 column equilibrated with 0.1 M MES (pH 6.5) to remove adventitious iron and the iron concentrations of the eluted proteins determined from their absorbance at 340 nm. The protein samples and the control were then diluted with 0.1 M MES (pH 6.5) to give 1 mL solutions with a final iron concentration of 20 μM (0.17 μM wild-type BFR, 2.4 μM Glu128Arg/Glu135Arg BFR), 10 μL of 10 mM Tiron was added to give a final concentration of 100 μM Tiron (i.e., five Tiron molecules per Fe atom; earlier experiments using Fe^{3+} under the same conditions showed that one Fe^{3+} ion binds per two Tiron molecules), and the formation of Fe^{3+}−Tiron complexes was followed by monitoring the absorbance at 560 nm. The extinction coefficient for the Fe^{3+}−Tiron complex in 0.1 M MES (pH 6.5) was determined to be 4700 M^{-1} cm^{-1} by titrating 100 μM Tiron in 0.1 M MES (pH 6.5) with known concentrations of Fe^{3+}.

Samples for EPR were prepared in 100 mM MOPS (pH 7.0) and X-band EPR spectra measured at the University of East Anglia with a Bruker ER 200D spectrometer and at the University of Essex using a Bruker EMX spectrometer, both equipped with liquid helium flow cryostats. The concentrations of the paramagnetic centers were determined with reference to $CuSO_4$ concentration standards using the pure line shape EPR signals obtained either by subtraction with variable coefficients[54,55] (isoforms I and II of the rhombic Fe^{3+} ions) or by individual spectral simulation (high-spin and low-spin heme and the free radical). WINEPR SimFonia v1.25 (Bruker Analytishce Messtechnik) was used to simulate EPR spectra. For the desferrioximine (DFO)/HCl experiment, when it was not possible to use either of these techniques for obtaining pure line shapes, the procedure described by Svistunenko et al.[54,55] was employed. This procedure involved double integration of a series of spectra containing the overlapping signals in different proportions, and composing and solving a system of linear equations to obtain the double-integral values for the individual signals. The quantification of the $g = 4.3$ signals was performed at 100 K, since it is only at temperatures this high that the fraction of the rhombic Fe^{3+} centers detectable by EPR is exactly 1/3 of the total concentration, thereby removing the need for the zero-field splitting parameter D to be known.[41,56] To investigate removal of Fe^{3+} from the *R. capsulatus* subunit dimer, EPR samples were treated with DFO to a final concentration of 1 mM DFO and/or with HCl to a final pH ≈ 1.

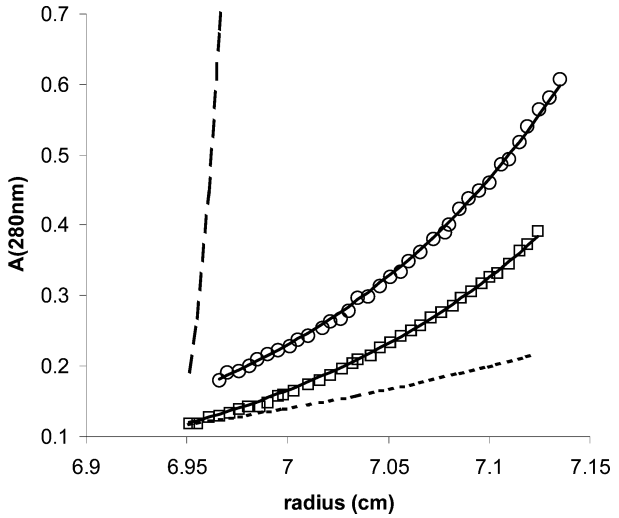

Figure 2. Sedimentation equilibrium data for nonheme iron free Glu128Arg/Glu135Arg *E. coli* BFR (□) and for protein containing nine nonheme Fe^{3+} ions per dimer (○). Both samples were 4 μM dimer in 0.1 M MES (pH 6.5) at 20 °C. Solid lines show curve fits as described in the Experimental Section; in both cases υ was set at 0.73 mL/g. The molecular mass of the nonheme iron free protein was determined to be 34.9 kDa, while that of the iron-loaded protein was 36.5 kDa. The latter value was unaffected by changing υ to compensate for the added iron as described in the Experimental Section. Dotted and dashed lines show predicted curves for molecular masses of 18.5 and 444 kDa, respectively, using data obtained for nonheme iron free protein.

Results

Properties of the Assembly Defective Forms of *E. coli* and *R. capsulatus* Bacterioferritins. Sedimentation equilibrium measurements showed that the Glu128Arg/Glu135Arg *E. coli* bacterioferritin behaved as a single species in the analytical ultracentrifuge with a molecular mass of 35−36 kDa (Figure 2). This indicates that the protein exists as a subunit dimer in 0.1 M MES (pH 6.5) consistent with previous studies of Glu128Arg/Glu135Arg *R. capsulatus* bacterioferritin that showed that it too is a dimer.[34,42] UV−vis spectra of the as-prepared Glu128Arg/Glu135Arg dimers showed both contained heme, though to different extents: the *R. capsulatus* protein typically contained 0.6−0.7 heme group per molecule, and the *E. coli* dimer typically contained up to 0.3 heme group per molecule. The variation in heme content probably reflects the amount of heme available in the cell relative to the overexpressed mutant BFR rather than any intrinsic differences between proteins. The Met52Ala/Glu128Arg/Glu135Arg *R. capsulatus* bacterioferritin was heme-free as prepared and did not bind added hemin, as expected since the Met52 side chains of adjacent subunits provide the two heme axial ligands in the wild-type protein. On the addition of Fe^{2+} to aerobic solutions of the variant bacterioferritins, a rapid increase in absorbance at 340 nm showed that the proteins catalyzed Fe^{2+} oxidation (Figure 3). At low ratios of added Fe^{2+} per BFR subunit the dimeric mutant and wild-type 24-mer proteins had similar time courses, indicating the presence of functional ferroxidase centers in the dimeric mutants. The time courses of Fe^{2+} oxidation for the *R. capsulatus* Glu128Arg/Glu135Arg and Met52Ala/Glu128Arg/Glu135Arg proteins were also the same (not shown), consistent with previous studies[36] of heme-containing and heme-free 24-

(53) Kim, I.; Hosein, H.-A.; Strongin, D. R.; Douglas, T. *Chem. Mater.* **2002**, *14*, 4874−4879.
(54) Svistunenko, D. A.; Sharpe, M. A.; Nicholls, P.; Wilson, M. T.; Cooper, C. E. *J. Magn. Reson.* **2000**, *142*, 266−275.
(55) Svistunenko, D. A.; Sharpe, M. A.; Nicholls, P.; Blenkinsop, C,; Davies, N. A.; Dunne, J.; Wilson, M. T.; Cooper, C. E. *Biochem. J.* **2000**, *351*, 595−605.
(56) Sun, S.; Chasteen, N. D. *Biochemistry* **1994**, *33*, 15095−15102.

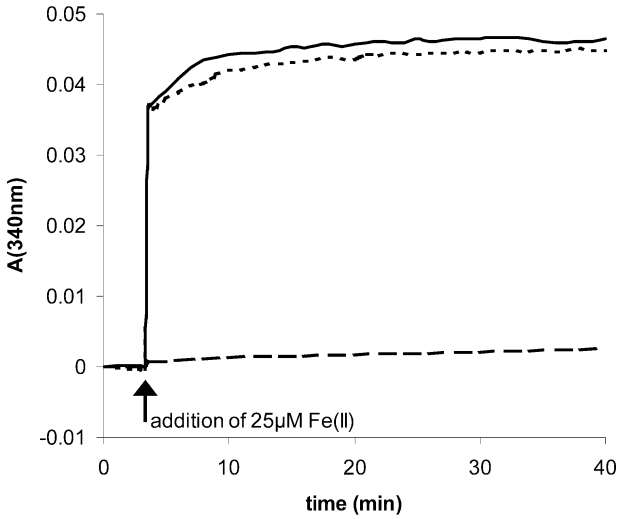

Figure 3. Oxidation of 25 μM Fe^{2+} in the presence of wild-type (WT) and Glu128Arg/Glu135Arg *E. coli* BFR. The solid line is for 0.5 μM WT *E. coli* BFR, and the dotted line is for 6 μM *E. coli* Glu128Arg/Glu135Arg BFR, both in 0.1 M MES (pH 6.5) at 25 °C. The dashed line is for the autoxidation of Fe^{2+} in 0.1 M MES (pH 6.5).

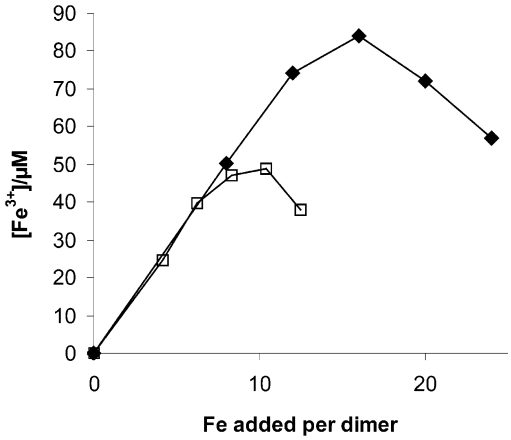

Figure 4. Graph showing the maximum amount of iron taken up by *E. coli* (□) and *R. capsulatus* (◆) Glu128Arg/Glu135Arg BFR dimers. Both proteins were 6 μM in 100 mM MOPS (pH 7.0) at 25 °C. Following each iron addition, oxidation was followed by measuring the absorbance at 340 nm, and when oxidation was complete, samples were centrifuged for 10 min at 14000 rpm and absorption spectra re-recorded. Fe^{3+} concentrations were estimated using extinction coefficients calculated from the 340 nm absorbance following oxidation of the first aliquot of Fe^{2+} ions, which did not lead to any precipitation.

mer *E. coli* bacterioferritin that showed that the heme did not play a role in oxidative aerobic uptake of Fe^{2+}. Addition of Fe^{2+} to the equivalent concentration (mg/mL) of bovine serum albumin (BSA) did not cause an increase in absorbance at 340 nm greater than that seen for autoxidation of Fe^{2+} in buffer only, showing that BSA did not catalyze oxidation of Fe^{2+}, consistent with the enhanced rate of Fe^{2+} oxidation seen for the subunit dimers, being a specific protein-catalyzed enhancement rather than a general nonspecific effect.

The maximum amounts of iron taken up by the *E. coli* and *R. capsulatus* BFR dimers were found to be different (Figure 4). When oxidation of added Fe^{2+} was complete following each addition of Fe^{2+} ions at pH 7 (100 mM MOPS, 25 °C), samples were centrifuged to remove any particulate material and absorption spectra re-recorded. Ferric ion concentrations were then estimated using extinction coefficients calculated from the 340 nm absorbance following oxidation of the first aliquot of Fe^{2+} ions, which did not lead to any precipitation. Assuming no precipitation of protein until after the maximum in the graphs is reached, the maximum nonheme Fe^{3+} content of the soluble dimer proteins is ~9 and ~15 for the *E. coli* and *R. capsulatus* proteins, respectively (Figure 4). The maximum nonheme Fe^{3+} content without precipitation determined by the procedure described in the Experimental Section at pH 6.5−7.0 was 8−10 Fe^{3+} ions per dimer for *E. coli* Glu128Arg/Glu135Arg BFR and 14−20 Fe^{3+} ions per dimer for *R. capsulatus* Glu128Arg/Glu135Arg BFR.

Fe^{3+} Ions Bind to the Subunit Dimer. Confirmation that nonheme iron added to just below the maximum loading possible was associated with the BFR subunit dimers (9 and 16 Fe^{3+} ions per molecule for the *E. coli* and *R. capsulatus* BFR dimers, respectively) was obtained by analytical ultracentrifugation (Figure 2) and gel permeation chromatography (not shown). The nonheme iron free subunit dimer of *R. capsulatus* Glu128Arg/Glu135Arg BFR and the subunit dimer containing 16 Fe^{3+} ions per dimer passed through a calibrated Sephacryl S100 HR gel permeation column with elution volumes equivalent to molecular masses of 32 ± 3.25 and 36 ± 3.25 kDa, respectively. For the subunit dimer containing 16 Fe^{3+} ions, the yellow/brown color associated with the Fe^{3+} ions traveled through the column with the protein component. Analysis of the eluted protein showed it contained 15 ± 0.5 Fe^{3+} ions per dimer, indicating loss of only ~6% of the nonheme iron on passage through the column. These data show that the nonheme iron is firmly associated with the subunit dimer, and since the molecular mass of the polypeptide component of the subunit dimer calculated from its amino acid sequence is 36452 Da, the gel permeation data also indicate that the *R. capsulatus* subunit dimer does not associate into high-order aggregates on the addition of Fe^{2+} and its oxidation to Fe^{3+}. Sedimentation equilibrium measurements with the *E. coli* subunit dimer demonstrated that it too remains as a monodisperse dimer in its iron-loaded form (Figure 2), and consistent with this, about nine Fe^{3+} ions remained associated with the subunit dimer following passage down a G25 Sephadex column.

Addition of hemin chloride to fully heme load the nonheme iron free *E. coli* subunit dimer prior to the addition of ferrous ammonium sulfate produced a nonheme iron content of about six Fe^{3+} ions per dimer prior to precipitation, indicating that the presence of heme does not materially affect the amount of Fe^{3+} that a dimer BFR can bind.

The *R. capsulatus* Subunit Dimer Associated Fe^{3+} Forms One or More Polynuclear Clusters. EPR spectra of samples of the subunit dimer of *R. capsulatus* Glu128Arg/Glu135Arg BFR containing variable amounts of nonheme Fe^{3+} contain seven well-defined signals (Figure 5). The features with g values of 2.88 and 2.33 are two of the three components of the low-spin heme iron,[57] the third component being relatively broad and having a g value of 1.45 (not shown). The features at g = 6.4 and g = 5.5 are from low amounts of high-spin heme Fe^{3+}. The relative concentration of the high-spin heme is negligible at <5% of the low-spin heme concentration. The g = 4.3 feature arises from nonheme Fe^{3+} in a rhombic environment. This

(57) Cheesman, M. R.; Kadir, F. H. A.; Al-Basseet, J.; Al-Massad, F.; Farrar, J.; Greenwood, C.; Thomson, A. J.; Moore, G. R. *Biochem. J.* **1992**, *286*, 361−367.

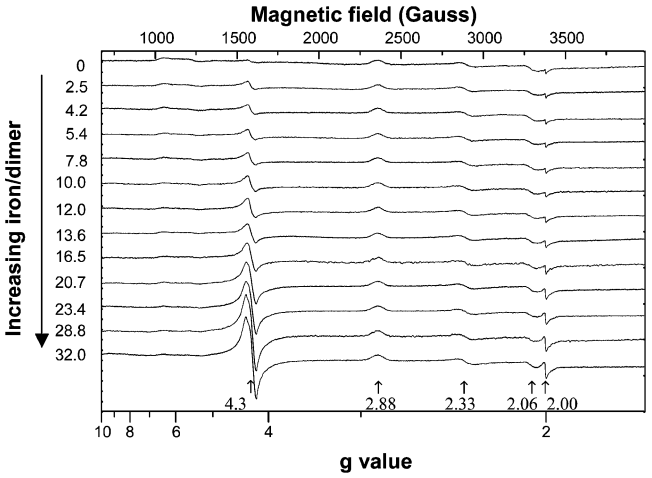

Figure 5. X-band EPR spectra of *R. capsulatus* Glu128Arg/Glu135Arg BFR containing different amounts of nonheme Fe^{3+}. The instrumental parameters were as follows: microwave frequency, 9.4713 GHz; microwave power, 0.8 mW; modulation amplitude, 2 G; time constant, 41 ms; scan rate, 2.38 G s^{-1}. Spectra were measured at 10 K. The ratio of added nonheme Fe^{3+} relative to the subunit dimer and the *g* factors of the EPR signals are indicated in the figure.

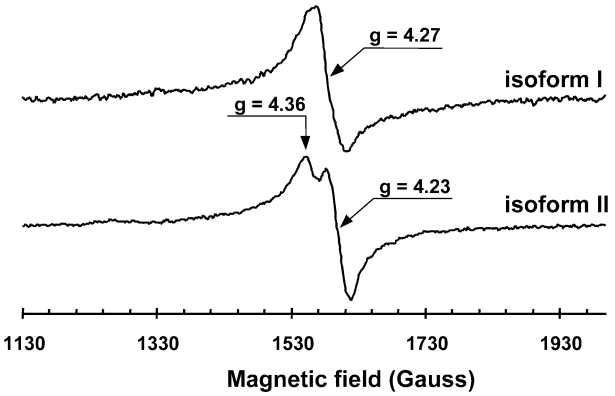

Figure 6. The two isoforms of the $g = 4.3$ signal extracted from the EPR spectra shown in Figure 5. First, the overall intensity of the $g = 4.3$ signal was corrected for the relative size of the low-spin heme EPR signal in the samples (as this is known to be invariant with iron loading). Isoform I was then obtained as the spectral difference between samples containing 12.0 and 0 Fe^{3+} ions per dimer, and isoform II as the difference between samples containing 32.0 and 13.6 Fe^{3+} ions per dimer. The principal *g* factors are indicated.

feature increases and changes its shape with iron loading because there are two overlapping signals that grow differently on iron loading. The individual signals, hereafter termed isoforms I and II, can be distinguished most clearly in difference spectra (Figure 6). The $g = 2.06$ signal is unassigned, and since it does not vary appreciably with iron loading, we do not consider it further here. The $g = 2.001$ signal is typical for a free radical. An axially symmetric free radical signal has been observed in EPR spectra of horse spleen ferritin (HoSF), and its intensity shown to increase with increasing amounts of Fe^{2+} added.[56] The identity of the HoSF radical has not been established, though a variety of amino acid centered radicals have been considered to be possible.[56] The radical signal for the BFR subunit dimer (Figure 5) is at very low concentrations compared to the species generating the $g = 4.3$ signals, and further work is required to establish whether the radical has a functional significance.

The apparent intensity of the $g = 4.3$ signal (Figure 5) did not increase with iron loading in a manner consistent with the formation of magnetically isolated Fe^{3+} species, because much

Table 1. EPR Quantitation of Fe^{3+} Species Generating a $g = 4.3$ Signal

no. of Fe^{2+} ions added per BFR subunit dimer	total nonheme Fe^{3+} concn (μM)	total rhombic Fe^{3+} ($g = 4.3$) concn (μM)			
		as prepared	DFO	HCl	DFO/HCl
13.6	190	3.5 [1.8%]	58 [31%]	nd	nd
16.5	231	5.3 [2.3%]	nd	nd	249 ± 29 [108%]
23.4	328	9.6 [2.9%]	nd	117 [36%]	nd

[a] nd = not determined.

of the iron is "invisible" to EPR spectroscopy. The iron chelator DFO binds a single Fe^{3+} ion tightly,[58] and acid denatures protein without rendering the ferric iron insoluble. Therefore, in isolation, or in combination, DFO and HCl should be able to render EPR-detectable invisible Fe^{3+}, by generating stable mononuclear magnetically isolated Fe^{3+} species. To confirm this was the case for the samples of BFR subunit dimer, DFO, HCl, and HCl with DFO were added to selected samples. The sample chosen for the DFO/HCl treatment had the same iron loading as that used for the gel filtration experiment. The acidification of the BFR samples, and the addition of DFO, caused significant increases in the intensity at $g = 4.3$ (Table 1), with the DFO/HCl treatment producing a $g = 4.3$ signal accounting for all the nonheme iron present in the sample. The key observation from Table 1 is that little of the nonheme Fe^{3+} present in the subunit dimer samples contributes to the $g = 4.3$ intensity in the absence of acid or DFO. Since the UV−vis absorbance of the iron-loaded subunit dimer showed that all the added Fe^{2+} had been oxidized to Fe^{3+}, the lack of sufficient EPR intensity at $g = 4.3$ indicates that the Fe^{3+} was not magnetically isolated and that coupling of electron spins had reduced the signal intensity. Similar observations have been made in EPR studies of intact 24-mer HoSF[56,59,60] and Fe^{3+}-containing frataxin multimers,[61] which showed that oxidation of added Fe^{2+} did not produce $g = 4.3$ signals with sufficient intensity to account for all the Fe^{3+} present. Quantification of the two $g = 4.3$ signals as a function of iron loading, by the procedure of Svistunenko and colleagues,[54,55] extended the conclusion from the DFO/HCl experiment (Table 1) by showing that, at the most, only 3% of the Fe^{3+} produced from the added Fe^{2+} was EPR-detectable (Figure 7). This quantitation also revealed that whereas the signal of isoform I appeared immediately on the addition of Fe^{2+}, the signal of isoform II did not appear until 16 Fe^{2+} ions per BFR subunit dimer had been added.

EPR spectra of *R. capsulatus* BFR subunit dimer samples containing from 12 to 32 nonheme Fe^{3+} ions per dimer were measured over the temperature range from 4.2 to 150 K (not shown). Signals additional to those shown in Figure 5 were not observed. Previous EPR measurements of intact ferritins[62−64]

(58) Telford, J. R.; Raymond, K. N. In *Comprehensive Supramolecular Chemistry*; Atwood, J. L., Davies, J. E. D., MacNicol, D. D., Voegtle, F., Eds.; Elsevier: Oxford, 1996; Vol. 1, pp 245−266.
(59) Chasteen, N. D.; Antanaitis, B. C.; Aisen, P. *J. Biol. Chem.* **1985**, *260*, 2926−2929.
(60) Hanna, P. M.; Chen, Y.; Chasteen, N. D. *J. Biol. Chem.* **1991**, *266*, 886−893.
(61) Adamec, J.; Rusnak, F.; Owen, W. G., Naylor, S., Benson, L. M.; Gacy, A. M.; Isaya, G. *Am. J. Hum. Genet.* **2000**, *67*, 549−562.
(62) Boas, J. F.; Troup, G. J. *Biochim. Biophys. Acta* **1971**, *229*, 68−74.
(63) Weir, M. P.; Peters, T. J.; Gibson, J. F. *Biochim. Biophys. Acta* **1985**, *828*, 298−305.
(64) Deighton, N.; Abu-Raqabah, A.; Rowland, I. J.; Symons, M. C. R.; Peters, T. J.; Ward, R. J. *J. Chem. Soc., Faraday Trans.* **1991**, *87*, 3193−3197.

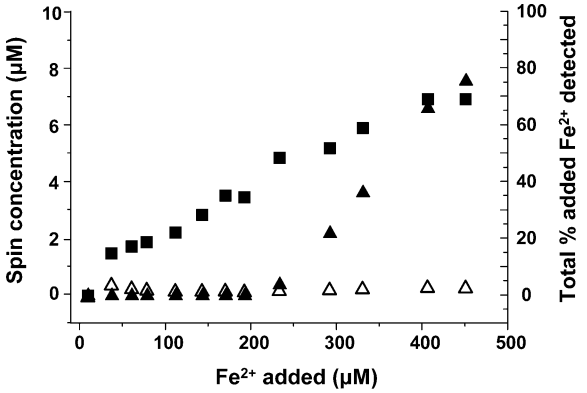

Figure 7. Concentrations of the two isoforms of the rhombic Fe^{3+} centers (isoform I with $g = 4.27$ and isoform II with $g = 4.36$ and $g = 4.23$; see Figure 6) as a function of iron added. The spin concentrations of isoforms I and II are indicated by ■ and ▲, respectively, and the total percentage of added Fe^{2+} detected as Fe^{3+} is indicated by △.

and BFR[57] containing large amounts of core Fe^{3+} identified signals that were absent at 4.2 K and present at temperatures of 10−150 K. A full theoretical description of these relatively high temperature signals has not been reported, but it is clear that their properties are connected with the formation of much larger polynuclear Fe^{3+} particles than those we believe are present in the BFR subunit dimer samples. The absence of similar signals from the EPR spectra of the Fe^{3+}-containing BFR subunit dimer is consistent with the gel permeation experiment showing that the subunits do not associate in the presence of Fe^{3+} to allow formation of particles of Fe^{3+} containing more than 16 Fe^{3+} ions.

The observation of two isoforms for the Fe^{3+} species giving rise to the $g = 4.3$ EPR signal (Figure 6) indicates that there are at least two electronically distinct Fe^{3+} centers. Since the maximum loading of soluble *R. capsulatus* Glu128Arg/Glu135Arg BFR with nonheme iron is 14−20 Fe^{3+} ions per molecule, isoform I must be associated with soluble BFR while isoform II may be associated with precipitated protein. Such EPR signals as those of isoforms I and II do not arise from the μ-oxo-bridged di-Fe^{3+} ferroxidase center,[41,59,60] and though they may arise from magnetically isolated Fe^{3+} ions, their intensities do not support this interpretation: even in the sample with 32 Fe^{3+} ions added per subunit dimer only ∼1.5% of the total Fe^{3+}, i.e., ∼0.5 Fe^{3+} ion per molecule, is detectable as each of the isoforms. An alternative explanation for these signals is that they arise from Fe^{3+} at the periphery of polynuclear clusters, where they are not magnetically coupled to other Fe^{3+} ions.

The BFR Subunit Dimer Associated Polynuclear Fe^{3+} Is Not Fully Accessible to Chelators. As noted above (Table 1), ∼69% of the Fe^{3+} associated with the DFO-treated *R. capsulatus* BFR subunit dimer containing an average of 13.6 Fe^{3+} ions per molecule was polynuclear, corresponding to ∼9.4 magnetically coupled Fe^{3+} ions per molecule, on average. Assuming that both ferroxidase centers of each subunit dimer were occupied by Fe^{3+}, this indicates that ∼5.4 Fe^{3+} ions were on the surface of the subunit dimer and not removed by DFO. This indicates that this surface-associated Fe^{3+} is relatively tightly bound to the protein, and thus not simply adventitiously bound. To determine whether there were kinetic barriers to the removal of the surface-associated Fe^{3+} by DFO, the time dependence of the formation of the colored complex formed between Fe^{3+} and the chelating ligand Tiron was monitored at 560 nm (Figure 8).

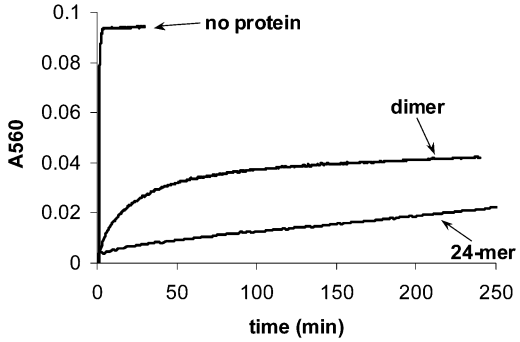

Figure 8. Increase in absorbance at 560 nm with time following the addition of 100 μM Tiron (final concentration) to 20 μM Fe^{3+}, 0.17 μM *E. coli* wild-type BFR containing 20 μM Fe^{3+}, and 2.4 μM *E. coli* Glu128Arg/Glu135Arg BFR containing 20 μM Fe^{3+}, all in 0.1 M MES buffer (pH 6.5) at 25 °C.

In this experiment, both proteins retained the equivalent of two Fe^{3+} ions per subunit on the basis of the extinction coefficient determined for Fe^{3+}−Tiron mixtures in 0.1 M MES buffer (pH 6.5) at 25 °C using standard iron solutions after 12 h of exposure to Tiron. The retained Fe^{3+} is presumably located in the ferroxidase centers. The Fe^{3+} in the subunit dimer is more accessible than in the 24-mer, but it is still tightly bound by the protein, as shown by the slow progress of chelation by Tiron compared to that of iron not associated with BFR (Figure 8).

General Discussion

The Bacterioferritin Subunit Dimers Contain Nucleation Sites for Polynuclear Fe^{3+} Species. The results show that Fe^{2+} added to the bacterioferritin subunit dimers becomes oxidized and remains associated with the protein in one or more magnetically coupled, and hence polynuclear, forms. The sedimentation equilibrium and gel permeation experiments and the lack of turbidity at iron:protein ratios of less than 8−10 and 14−20 Fe^{3+} ions per *E. coli* and *R. capsulatus* subunit dimer, respectively, indicates that one or more clusters of nonheme Fe^{3+} are bound to the subunit dimers, and the slow removal of this subunit-associated Fe^{3+} indicates that it is not adventitiously bound to the protein surfaces. Thus, it seems likely that each subunit dimer contains one or more nucleation sites for formation of polynuclear Fe^{3+} species. This is the first clear experimental support for the long-held view that the inner surfaces of bacterioferritins do contain nucleation centers for the mineral cores, something that has also been assumed for other ferritins though there is limited experimental support for this.[65]

The location of possible sites at which clusters of Fe^{3+} could be bound is assisted by the X-ray structures of *E. coli*[38] and *R. capsulatus*[43] bacterioferritins. These reveal that the surface of each subunit contains a patch of acidic residues close to the edge of the ferroxidase center ligands exposed to solvent (Figure 9). These residues—Glu46, Glu47, Asp/Glu50, and Asp126—would form part of the inner surface within the central cavity of the 24-meric structure, and thus not be exposed to the bulk solvent. However, a consequence of the subunit dimer not associating into a 24-meric structure is that these residues are

(65) Yang, C.-Y.; Meagher, A.; Huynh, B. H.; Sayers, D. E.; Theil, E. C. *Biochemistry* **1987**, *26*, 497−503.

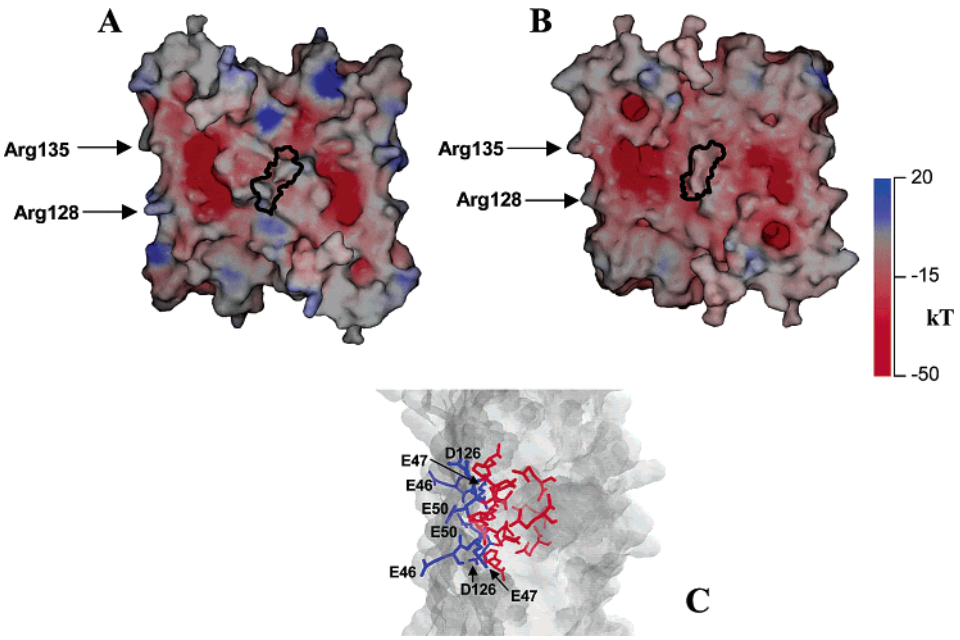

Figure 9. Calculated electrostatic surface potentials of the heme-containing and nonheme iron free *E. coli* Glu128Arg/Glu135Arg (A) and *R. capsulatus* Glu128Arg/Glu135Arg (B) BFR dimers viewed from the side that forms the inner surface of the 24-mer structure. The thick black line in the center of each structure represents the position of the heme group. Side view of the *R. capsulatus* Glu128Arg/Glu135Arg BFR dimer showing the ferroxidase center ligands in red and the carboxylic acids proposed to act in core nucleation (see the text) in blue (C). Coordinates for the *E. coli* and *R. capsulatus* Glu128Arg/Glu135Arg dimers were created using PDB coordinates 1bcf and 1jgc, respectively, with the coordinates of the *R. capsulatus* subunit dimer obtained by orienting the coordinates of its subunit monomer onto those for the *E. coli* dimer. Residues 128 and 135 of both subunits in each dimer were altered to arginines and the manganese ions present in the *E. coli* structure removed. (A) and (B) were created with SPOCK,[67] and the electrostatic calculations were done using a temperature of 25 °C and an ionic strength of 0.15 M. The heme propionates were assumed to be un-ionized in the electrostatic calculations because the experiments reported in this paper showed that the loading of nonheme iron was not significantly affected by the presence of heme. Moreover, they have an intrinsic pK_a of ∼5.6, which is often substantially raised in proteins by environmental effects.[68] (C) was generated with Swiss PDB Viewer 3.7b2.[69]

now exposed to bulk solvent. Thus, a plausible mechanism for formation of one or more polynuclear Fe^{3+} clusters is that Fe^{2+} binds at the ferroxidase center and is oxidized to Fe^{3+} with formation of a μ-oxo-bridged Fe^{3+} dimer, followed by the accretion of Fe^{2+} onto the surface of the protein, where it binds to the carboxylate groups and is oxidized to Fe^{3+}, either through direct reaction with O_2 in a mineral surface reaction or indirectly with the involvement of the ferroxidase center.[17,41] Comparison of the structure of the *E. coli* Glu128Arg/Glu135Arg BFR with that of the corresponding *R. capsulatus* mutant BFR supports this general scheme. As described above, both mutant bacterioferritins remain as subunit dimers on binding Fe^{3+}, but the maximum amounts of Fe^{3+} they can bind are different: the *E. coli* protein 8−10 Fe^{3+} ions per dimer and the *R. capsulatus* protein 14−20 Fe^{3+} ions per dimer. Consistent with this variation, the *E. coli* dimer has a less negatively charged surface than does the *R. capsulatus* dimer (Figure 9A,B). This difference arises partly because whereas residues 47, 50, and 126 are carboxylic acids in both proteins, residue 46 is glutamate in *R. capsulatus* BFR but histidine in the *E. coli* protein. Also, *E. coli* BFR has a greater number of lysine residues on its inner surface than does *R. capsulatus* BFR. Comparison of 37 BFR sequences in the Swiss-Prot/TrEMBL database show that residue 46 is variable, residue 47 is glutamate in 30 BFRs, residue 50 is aspartate or glutamate in 32 BFRs, and residue 126 is aspartate or glutamate in 28 BFRs. We do not know that all of these bacterioferritins lay down cores, but it is suggestive that residues 47, 50, and 126 have a high degree of conservation. These inner surface charges may have a role in guiding incoming Fe^{2+} into the central cavity through the channels as well as in nucleating a core particle. The importance of electrostatic gradients in ferritins has previously been pointed out by Douglas and Ripoll,[66] who proposed that gradients coincident with the channels through the 24-mer shells of animal ferritins are important for guiding incoming Fe^{2+} to the nucleation center(s). Macedo et al.[39] have also identified clusters of negative charge on both the inner and outer surfaces of the *Desulfovibrio desulfuricans* bacterioferritin and suggest that these provide an alternative route for iron to access the protein core.

What Is the Chemical Form of the Polynuclear Fe^{3+} Species, and What Are the Chemical Steps Leading to Their Formation? These are the key questions whose answers will provide insight into core formation in intact ferritins. The detailed chemical steps to the formation of the polynuclear Fe^{3+} cores of ferritins have not been established, but the growth of polynuclear crystallites of Fe^{3+} in Cl^--containing aqueous solutions provides guidance as to the events that may be occurring.[3] Even at an early stage of polynuclear growth in this system involving 2−9 Fe^{3+} ions in a cluster, modeling the growth process required 61 distinct polynuclear species. By providing a nucleation template in our experiments in the form of the BFR subunit dimers, the number of polynuclear species formed may have been reduced considerably. However, it is not yet clear whether the polynuclear Fe^{3+} species are amor-

(66) Douglas, T.; Ripoll, D. R. *Protein Sci.* **1998**, *7*, 1083−1091.
(67) Christopher, J. A.; Baldwin, T. O. *J. Mol. Graphics* **1998**, *16*, 285.
(68) Moore, G. R.; Pettigrew, G. W. *Cytochromes c: Evolutionary, structural and physicochemical aspects*; Springer-Verlag: Berlin, 1990; pp 12−14 and 348−354.
(69) Guex, M.; Peitsch, M. C. *Electrophoresis* **1997**, *18*, 2714−2723. Also see http://www.expasy.org/spdbv/.

phous or ordered. Attempts to obtain crystals of Fe^{3+}-containing subunit dimers suitable for X-ray crystallography are under way, and if suitable crystals can be obtained, X-ray crystallography should provide an answer to this. Current investigation of the chemical steps leading to the formation of the polynuclear Fe^{3+} species is focused on the issue of whether incoming Fe^{2+} attached to the surface of the subunit dimer is oxidized by O_2 directly or whether the ferroxidase center plays a role in its oxidation, as occurs in native 24-mer BFR but not in other ferritins for which the mineral surface plays a major role in coupled processes of Fe^{2+} oxidation and O_2 reduction. What is clear, however, is that for the first time a form of ferritin has been obtained in which there is unambiguous chemical evidence that its inner surface contains a nucleation site for core formation, thus indicating that ferritins are not simply vessels that contain polynuclear Fe^{3+} species isolated from the bulk surroundings in which hydrolysis of Fe^{3+} and formation of its polynuclear species occur independent of the protein.

Acknowledgment. We thank the Wellcome Trust and the Biomolecular Sciences Panel of the BBSRC for supporting work on ferritins at the University of East Anglia, the Joint Infrastructure Fund for equipment, the Wellcome Trust for their support of the University of Essex Biomedical EPR facility, and the EPSRC for a studentship for S.A.M. We are also grateful to D. Cobessi (Lawrence Berkeley National Laboratory, California) for generously supplying coordinates of the *R. capsulatus* BFR structure prior to publication, the acrobatic A. G. Mauk (Vancouver) for help with locating publications and useful discussions, and C. M. Hesketh (Norwich) for helpful discussions concerning iron uptake into ferritins.

JA036483Z